**Supplemental Digital Content**

Figure S-1. Computational model of an adult human airway network derived from a thoracic CT scan. (A) The model consisted of 60,494 airway segments and 30,243 terminal acini, obtained by algorithmic generation of peripheral airway segments after initial central airways segmentation. Mechanical impedance models for (B) airway segments and (C) viscoelastic acini. Electrical circuit analogs are used to represent resistive, inertial, and elastic elements. Acinar tissue viscoelasticity was modeled using a constant phase element.

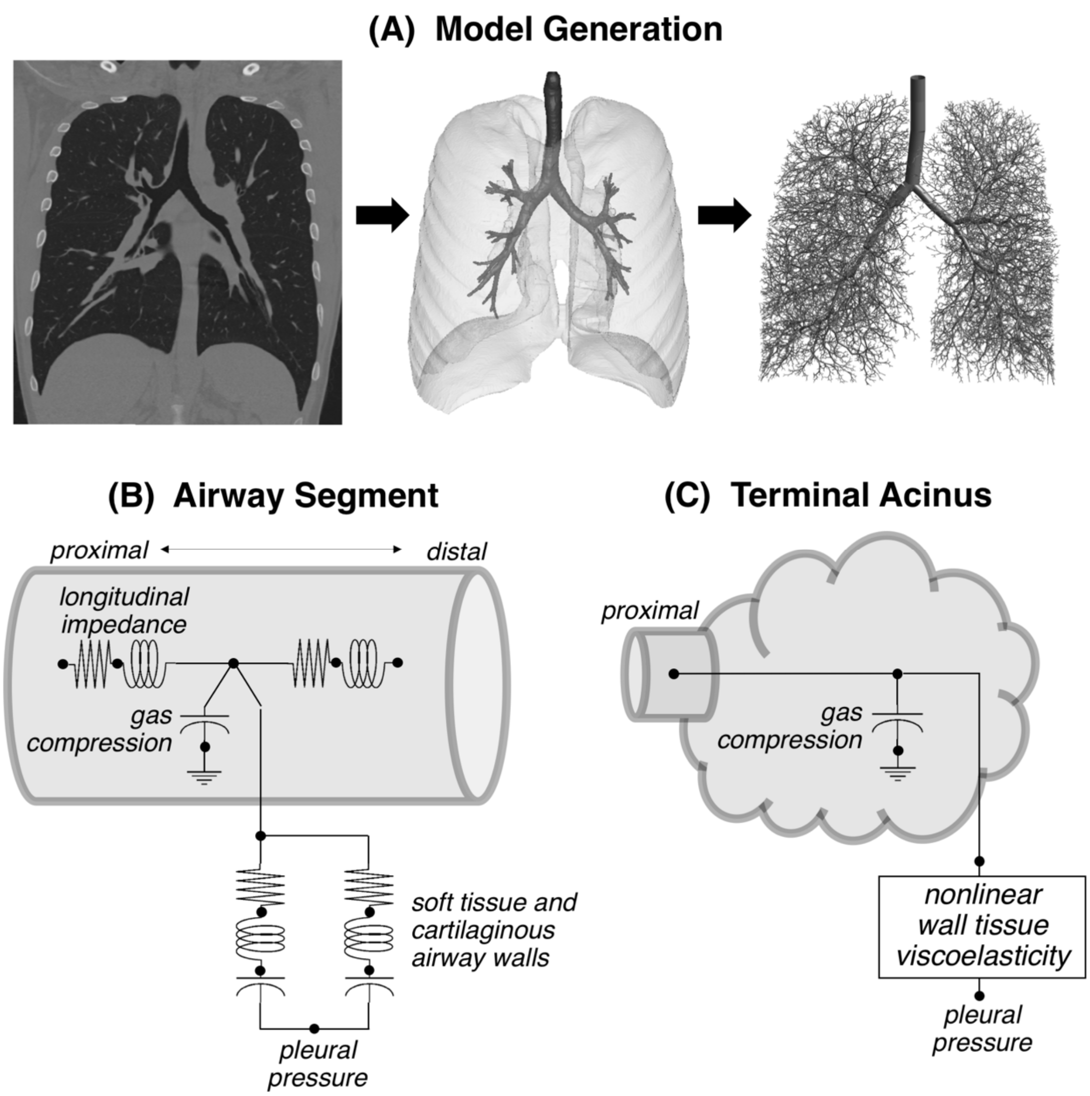

Figure S-2. Total lung resonant frequency, corner frequency, and quality factor as functions of lung size and injury severity. Increasing injury severity is shown from the healthy condition (light grey) to severe injury (black). Error bars denote standard deviation from ten random spatial patterns of lung tissue stiffness and derecruitment. Points connected by lines represent isometrically scaled lungs, relative to the adult model. Triangles indicate the resonant and corner frequencies for the lung model as scaled to neonatal proportions.

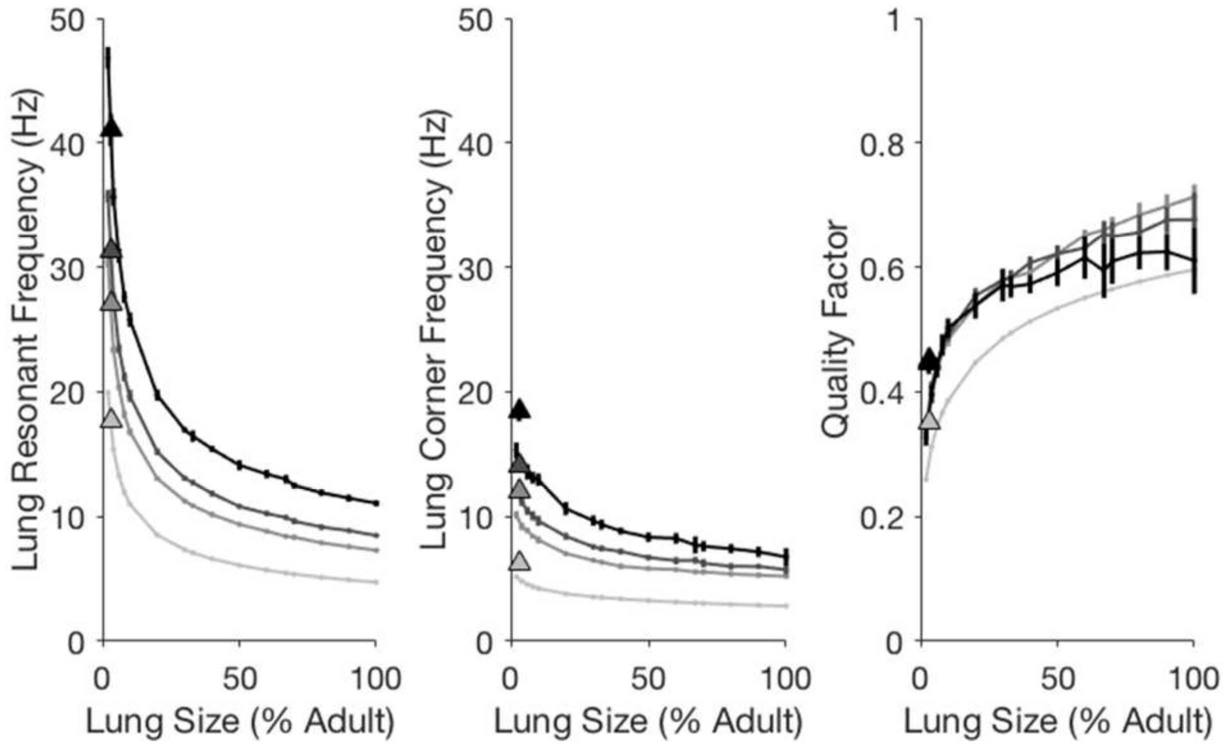

Table S-1. Selected healthy lung models constructed according to deadspace ($V_D$) and total acinar volume ($V_A$), and resulting mechanical properties: resonant frequency ($f_{res}$), airways resistance ($R_{aw}$), airways inertance ($I_{aw}$), tissue hysteresivity (η), and tissue elastance ($H$).

| Model | $V_D$ (mL) | $V_A$ (mL) | $V_D$:$V_A$ (%) | $f_{res}$ (Hz) | $R_{aw}$ ($cmH_2O$ s $L^{-1}$) | $I_{aw}$ ($cmH_2O$ $s^2$ $L^{-1}$) | η | $H$ ($cmH_2O$ $L^{-1}$) |
|---|---|---|---|---|---|---|---|---|
| 100% Adult | 155.6 | 3515.7 | 4.4 | 4.7 | 0.46 | 0.017 | 0.11 | 12.3 |
| 33% Adult | 51.3 | 1172.1 | 4.4 | 7.1 | 1.27 | 0.025 | 0.12 | 37.0 |
| 4% Adult | 6.2 | 140.7 | 4.4 | 15.4 | 9.27 | 0.049 | 0.15 | 303.8 |
| Neonate | 6.2 | 104.6 | 6.0 | 17.7 | 9.50 | 0.049 | 0.14 | 404.8 |

### *Scaling laws for global lung mechanics*

The $R_{aw}$, $I_{aw}$, $H$, and $\eta$ parameters were estimated by fitting a 4-parameter 'inverse' model of the lungs to simulated impedance spectra from our 'forward' anatomic model, at frequencies ranging between 0.2 Hz and $f_{res}$ for each model:

$$Z_{\mathrm{mod}}(f) = R_{\mathrm{aw}} + j2\pi f I_{\mathrm{aw}} + \frac{(\eta - j)H}{(2\pi f)^{\alpha}} \qquad \text{Equation 1}$$

where $\alpha = (2/\pi)\tan^{-1}(1/\eta)$. Model regressions were performed by a nonlinear gradient descent technique that minimized the sum of squared differences between simulated and model-predicted impedance spectra.

Figure S-3. Total lung tissue elastance $H$ (▲, cmH$_2$O L$^{-1}$), resonant frequency $f_{res}$ (●, Hz), airway resistance $R_{aw}$ (▼, cmH$_2$O s L$^{-1}$), tissue hysteresivity η (■, dimensionless), and airway inertance $I_{aw}$ (♦, cmH$_2$O s$^2$ L$^{-1}$) scale as power-law functions (—) of lung size ($V$, %) in isometrically scaled models of the adult lung (filled symbols). Values for the neonatal lung model (open symbols) are shown for comparison.